Exploring the effects of waxing in soft soils

K. Ouyang[1], J.A. Pineda[2], L.P. Suwal[3]
Priority Research Centre for Geotechnical Science and Engineering, The University of Newcastle Australia, Newcastle, Australia,
email[1]: Kaiwen.ouyang@uon.edu.au, email[2]:Jubert.pineda@newcastle.edu.au,
email[3]:Laxmi.suwal@newcastle.edu.au

ABSTRACT: This paper explores the consequences of the thermal loading caused by waxing, used in practice to seal tube and block specimens, on the quality of natural soft soils specimens. The details of pilot experimental and numerical programs are presented. It includes a waxing test carried out on a natural soft clay from the National Soft Soil Field Testing Facility (NFTF) located in Ballina (NSW, Australia). Experimental results were used to calibrate a numerical model aimed at estimating the thermal field imposed by the thermal loading due to waxing. Estimations of maximum excess pore pressure generated by the thermal loading are presented in discussion. Potential impacts of the thermal loading on the mechanical parameters obtained from laboratory tests which are used in geotechnical design are also discussed.

Keywords: soft clay, thermal effect, sampling,

1. Introduction

In geotechnical practice, wax is widely used to seal tube and block specimens after sampling[1]. A conventional procedure of wax sealing is to pour the melted wax directly on exposed surfaces of tube and block specimens. Once the wax cools down and solidified, a barrier is formed to prevent moisture losses within the samples. Despite of its proved efficiency as sealing method [2-4], there is implicitly assumed that waxing does not alter the soil properties with the exception of the soil located close to the top and bottom ends [1]. This empirical procedure neglects the possible impact of the thermal gradient generated by waxing on the mechanical properties of the sampled soil.

Over the past decades, the need for developing sustainable facilities to dispose nuclear waste has promoted vast amount of research studies that have focused on understanding the behaviour of natural and compacted geomaterials when subjected to thermal, hydraulic and mechanical actions [5-12]. Knowledge gained from those studies may now be applied to evaluate other problems such as the thermal gradient induced by waxing as well as the excess pore water pressure and any soil deformation caused by the thermal loading in tube and block specimens of soft soils (see Figure 1).

This paper presents preliminary results of an experimental and numerical study aimed at evaluating the influence of the thermal gradient caused by waxing on tube specimens of soft clay. A simple analytical model is adopted in this study to predict the maximum excess pore water pressure generated by the thermal loading.

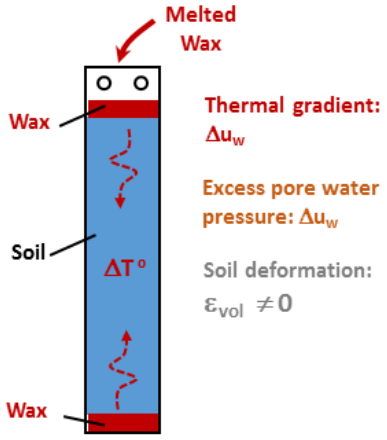

Figure 1 Thermal disturbance caused by wax sealing

2. Materials

The soil tested is Ballina clay obtained from the National Soft Soil Field Testing Facility (NFTF) located at the town of Ballina, north New South Wales (Australia). Ballina clay represents the estuarine soft soil deposits commonly encountered in south and east Australian coastlines. Typical features of these deposits are very low undrained shear strength, high compressibility, low water permeability and the presence of weak soil structure (fabric) easily destroyed when the yield stress is exceeded [13]. Ballina clay is mainly composed by kaolinite, illite, amorphous minerals and interstratified illite/smectite [13,14].

The soil tested in this paper was retrieved between 9.3 m and 9.6 m depth using a fixed-piston sampler (89 mm in diameter) [14]. Table 1 presents some basic properties of the soil. It has a natural water content around 111.7 %, which is close to its liquid limit (115 - 119.2 %). The void ratio of the natural soil is around 3.

Table 1. Basic properties of Ballina clay

Property	Description
Natural water content	102.4-111.7%
Liquid limit	115-119.2%
Plastic limit	48.9-49.8%
Dry density (Mg/m^3)	0.70-0.72
Void ratio	2.99
Mineral composition	Kaolinite:24.5% Illite:18% Amorphous mineral: 18% Illite/smectite:12% Quartz:10% Pyrite:6%

3. Thermal loading test

To evaluate the effects of waxing within a tube specimen, a pilot thermal loading test was performed. The test was carried out using the top part (203 mm in length) of a natural tube sample retrieved with the fixed piston sampler described above. Although the top end of the tube was previously waxed during the sampling campaign, this layer of solidified wax and the upper 5 mm of soil were removed prior to the thermal loading test. Thermocouples were installed at two locations within the soil (2/2* and 3/3*) as shown in Figure 2. Temperature variation was measured at the center of the sample but also at the tube wall. An additional pair of thermocouples (4/4*) were used to measure the temperature inside the wax. After the installation of the thermocouples, melted wax was poured directly on the top of the specimen to form a layer of 15 mm in thickness. Temperature was logged during the cooling stage until it reached the laboratory room condition ($T_o \approx 22$ °C).

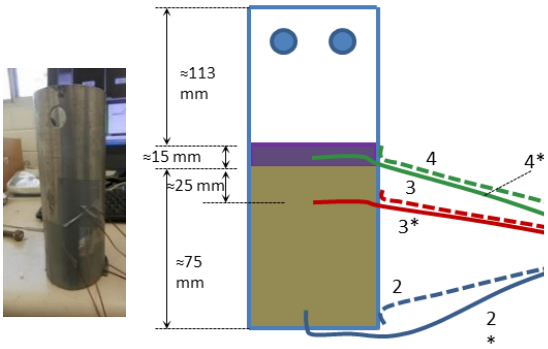

Figure 2 Experimental setup for the thermal loading test

4. Experimental results

Figure 3 presents the evolution of temperature with time measured at different locations in the tube sample. Temperature in the wax reached a maximum value of 85 °C after pouring. Then, it reduced gradually to room conditions ($T_o \approx 22$ °C) in less than one day. A maximum temperature of 34 °C was measured by thermocouple 3*, located below the wax/soil interface. At the bottom of the sample, a maximum temperature of 28 °C was recorded. The wax layer was removed after 1 week and clear traces of soil oxidation were detected.

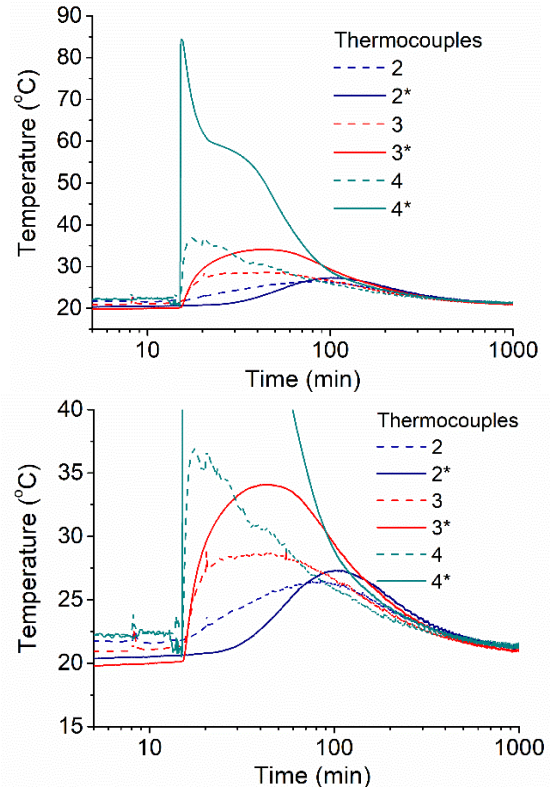

Figure 3 Temperature variation with time after waxing

5. Simulation of thermal loading caused by waxing

To get a better understanding of the evolution of the thermal gradient generated by waxing in tube sample, a simple numerical modelling of the thermal loading was performed using the finite element analysis program ABAQUS FEA 6.14. For the sake of simplicity, it was assumed that conduction is the only factor that controls the temperature field within the sample. Therefore, the basic energy balance equation could be simplified as:

$$\int_V \rho \dot{U} dV = \int_S q dS - \int_V r dV \qquad (1)$$

where V is the volume of the material with surface area of S, ρ is the density of the material, $\dot{U}$ is the material time rate of the internal energy, q is the heat flux per unit area of the body, r is the heat supplied internally into the body per unit volume.

The heat flux q and the internal energy U are calculated via following equations respectively:

$$q = -\lambda \nabla T \qquad (2)$$

$$dU = c(T)dT \quad (3)$$

where λ is the thermal conductivity of the material, ∇T is the thermal gradient, and c is the heat capacity of the material. For solid materials, heat capacity is constant. However, for materials that experience phase change during the simulation process, the heat capacity varies with temperature in consideration of latent heat.

In this study, the phase change behaviour is described using following equation:

$$c(T) = \begin{cases} c & (T > T_L \text{ or } T < T_s) \\ c + \dfrac{L}{T_L - T_S} & (T_s < T < T_L) \end{cases} \quad (4)$$

where L is the latent heat, T_S and T_L are solidus and liquidus temperatures respectively. Equation 4 assumes that the phase change occurs within a specified temperature range (defined by the solid and liquid temperature), and the release of latent heat varies linearly with temperature. Table 2 summarizes the parameters of the materials adopted in the simulations.

Table 2 Thermal parameters for the materials

Material	Wax	S.S. tube	Soil
Heat capacity (10^3J/kg·K)	2.9[15]	0.502[16]	1.381[17]
Thermal conductivity (W/m·K)	0.25[18]	16[19]	1.5[20]
Density (kg/m^3)	900[21]	7480[22]	1348[13]
Latent heat (10^5J/kg)	2[23]	-	-
Solidus temperature (ºC)	50[23]	-	-
Liquidus temperature (ºC)	60[23]	-	-

For the boundary condition, two kinds of boundaries were used in the simulation, the adiabatic boundary and convective boundary. No heat flux is allowed at the adiabatic boundaries, while the heat flux at the convective boundaries is controlled by the convective equation:

$$q = c_{conv}(T - T_0) \quad (5)$$

where q is the heat flux at the boundary, c_{conv} is the convection coefficient at the boundary, T is the temperature at the boundary surface, and T_0 is the temperature of the environment.

The simulations of the waxing process were divided into 2 stages. In the first stage, simulation of the pilot test was performed to calibrate the boundary conditions based on the experimental results. The setup used in the numerical simulations is shown in Figure 4. A 2D axisymmetric analysis was performed. An adiabatic boundary was assigned to the symmetric axis, and the other boundaries were assigned with convective boundaries to simulate the heat loss from the system (soil+wax+tube) to the environment. Four-node linear heat transfer elements were adopted in the simulation. The element size for soil and wax was 1 mm, while for the stainless steel tube it reduced to 0.5 mm.

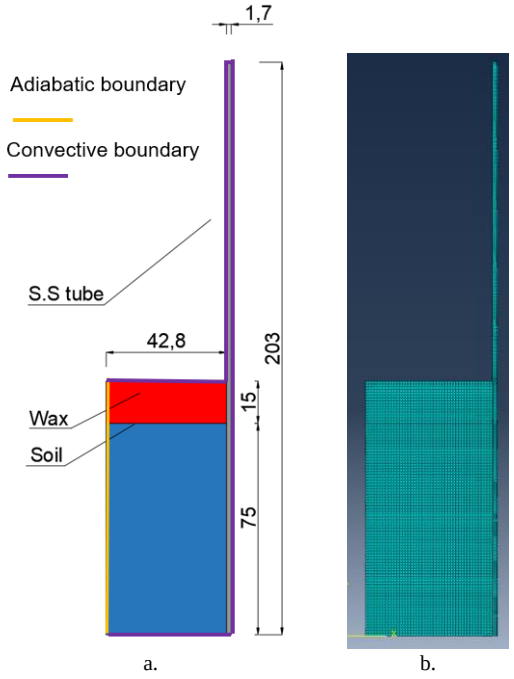

Figure 4 Simulation of the pilot waxing test (a). Geometrical settings and boundary conditions (b). Mesh setup of the numerical model

To simulate the pilot test, the initial temperature of the wax was set as 85ºC. The room temperature (i.e. environment temperature) and the initial temperature of the tube sample was set equal to 22 ºC. To simplify the heat transfer process between different materials, tie contact was assigned at the soil-wax, wax-tube and tube-soil interface. There was assumed no heat loss at those interfaces. Based on the temperature variation measured in the waxing test, a fitting exercise was followed to determine the value for the convection coefficient able to represent the experimental results. The best fitting was obtained for a value of $20\mathrm{W}/(\mathrm{m}\cdot\mathrm{K})$. As shown in Figure 5(a), the simulated temperature variation after waxing agrees well with the experimental results.

Figure 5(b) presents the maximum temperature estimated along the centerline of the specimen. At the soil-wax interface, the temperature of soil reaches 48 ºC. At the bottom of the sample, a maximum temperature of 30 ºC is estimated, indicating that the whole tube sample is affected by the thermal effects.

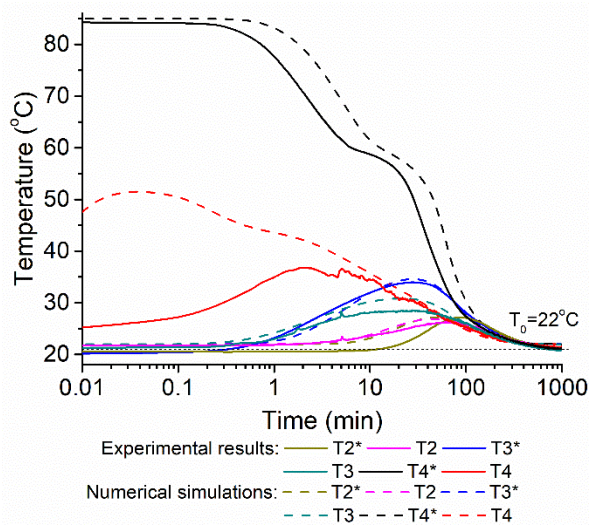

a.

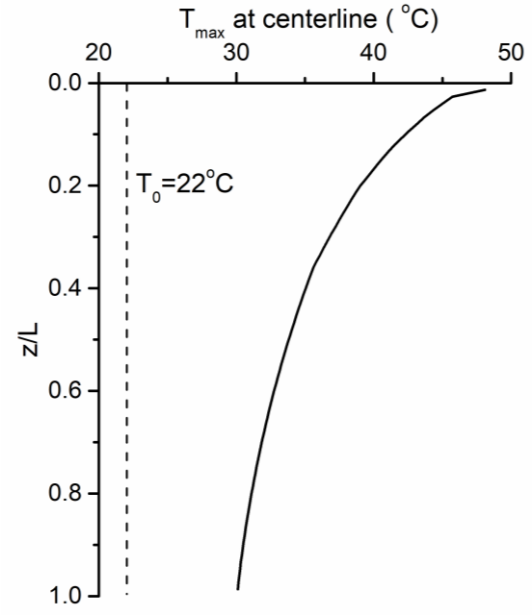

b.

Figure 5 Simulation of the waxing test. (a) Evolution of temperature with time. (b) Maximum temperature at centerline (L=75mm)

6. Parametric analysis

Based on the calibration above, a parametric analysis was then performed in order to evaluate: (i) the influence of the amount of heat applied to the system, which is controlled by the height of the wax layer, and (ii) the thermal field generated in samples of different sizes. The setups for the simulations are shown in Figure 6, in which half of a full tube specimen is considered.

In the first case, different heights of wax layer (namely 10mm, 30mm and 50mm) were numerically simulated to control the amount of heat applied to the system. Figure 7 shows the variation of the maximum temperature estimated along the centerline of the sample. As expected, with an increase in the heat input, the thermal gradient travels longer within the specimen. For the soil at the soil-wax interface, a maximum temperature of 48°C is observed. Under different heat input, the thermal disturbed zone ranges between 0.15 L and 0.25 L (L is the length of the tube), indicating that around half of the tube sample could be affected by the thermal loading if the thickness of wax layer is larger than 30mm.

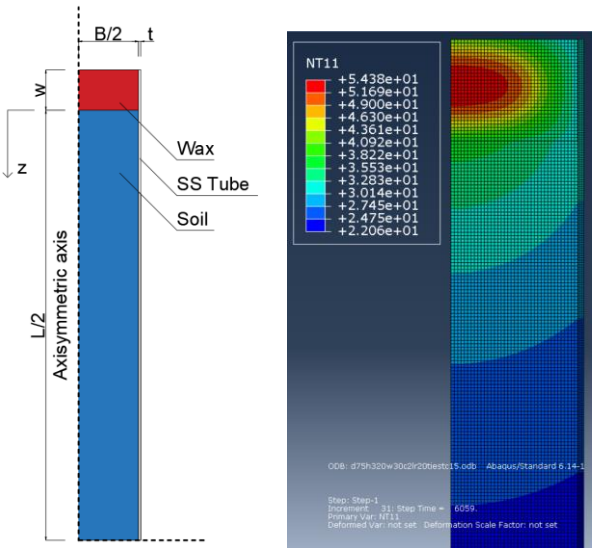

a. b.

Figure 6 Setup of parametric analyses (a) Model setup, (b) Generated thermal profile

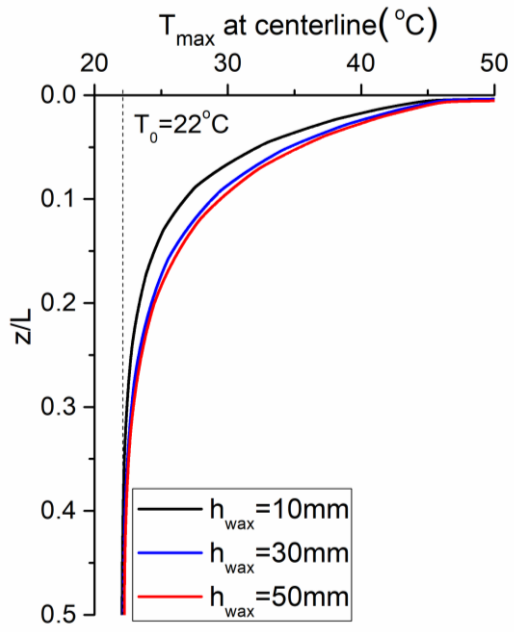

Figure 7 Parametric analysis: influence of heat input (L=700mm)

In the second set of numerical simulations, the same volume of heat was applied to tube specimens of different diameters to evaluate the influence of sampler type on the thermal gradient generated by waxing. To control the amount of heat, the volume

of the wax layer was maintained constant in all the simulations. The maximum temperature estimated at the centerline shown in Figure 8 indicates that for the same amount of heat input, sample diameter has limited effect on the thermal disturbed zones caused by wax sealing. Therefore, the influence of sampler type on the thermal disturbance is insignificant if the same heat is applied to the sample.

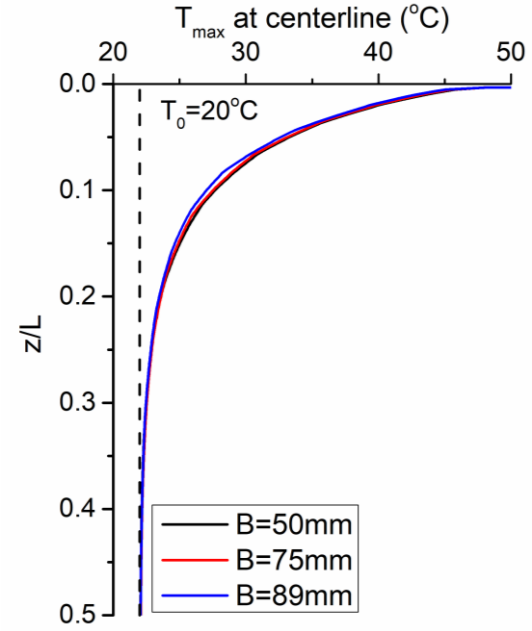

Figure 8 Parametric analysis: influence of sampler type (L=700mm)

7. Discussion

The experimental results and the numerical simulations presented above have showed the evolution of the thermal gradient caused by waxing in tube specimens of soft soil. Although the evolution of the excess pore water pressure caused by the thermal loading in tube specimens is also a concern, this aspect was not accounted for in the numerical simulations described above.

In practice, as the waxing process aims at preventing the moisture losses in the soil sample, it is reasonable to assume that undrained conditions prevail. Therefore, an excess pore pressure would be generated by the increase in temperature. Preliminary estimation of this pore pressure is performed here using Equation 6 [25]:

$$\Delta u_w = \frac{n\Delta T(\alpha_{solid} - \alpha_{water}) + \alpha_{st}\Delta T}{m_v} \qquad (6)$$

where n is the soil porosity, m_v is the volumetric compressibility of soil, α_{solid}, α_{water}, and α_{st} are the thermal expansion coefficients of soil particle, water and soil structure respectively. As suggested by Mitchel and Soga [25], the structural thermal expansion coefficient of the soil could be calculated given the plastic index (PI):

$$\alpha_{st} = 1 \times 10^{-4} e^{-0.014PI} \qquad (7)$$

Figure 9 shows the relationship between the excess pore water pressure and temperature obtained from Equations 6 and 7. Parameters listed in this figure were obtained from the characterization of Ballina clay described by Pineda et al. [13]. It can be seen that an increase in temperature cases a positive excess pore pressure of 0.46 kPa/ºC. Therefore, at the soil-wax boundary, where a maximum temperature of 48ºC has been produced (as shown in Figure 8), the excess pore pressure generated by waxing could reach 12 kPa. For a natural soft clay with values of undrained shear strength between 10-15 kPa [13] an increase in excess pore pressure of that amount may cause the failure of the soil located closer to the heating source but also modifications in soil fabric (due to moisture redistribution) along the entire specimen. This aspect is currently under investigation at the University of Newcastle.

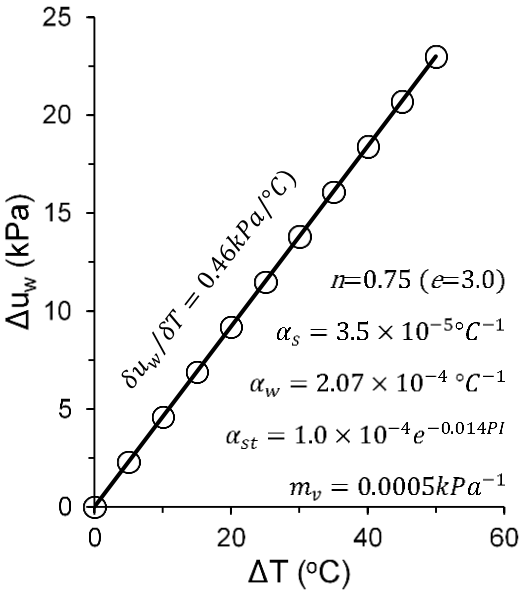

Figure 9 Excess pore pressure vs. temperature variation

8. Concluding remarks

The thermal effects caused by waxing in soft soils has been preliminarily evaluated in this paper. The heat transfer process after waxing was simulated based on experimental data. Possible influence of waxing on sample mechanical properties was also discussed.

The convection coefficient able to represent the thermal gradient caused by waxing in Ballina clay, found from back-analysis, was equal to $20\mathrm{W}/(\mathrm{m} \times \mathrm{K})$. Parametric analyses showed that half of the sample could be disturbed by waxing if the thickness of the wax layer is larger than 30mm, and the

sampler with smaller diameter is more vulnerable to the thermal disturbance. Possible excess pore pressure generated by the thermal loading, as well as potential disturbance in soil properties were also discussed based on previous literature. Further study is required to quantify the extent of the thermal disturbance for an improved understanding of sample quality.

References

[1] ASTM D3213-19, "Standard Practices for Handling, Storing, and Preparing Soft Intact Marine Soil", ASTM International, West Conshohocken, PA, 2019, www.astm.org

[2] Hvorslev, M.J., "Subsurface exploration and sampling of soils for civil engineering purposes". American Society of Civil Engineers, 521, 1949. .

[3] Lefebvre, G. and C. Poulin, "A new method of sampling in sensitive clay". Canadian Geotechnical Journal, 16(1): pp. 226-233, 1979.

[4] Rochelle, P.L., S. Leroueil, and F. Tavenas, "A technique for long-term storage of clay samples". Canadian Geotechnical Journal, 23(4): pp. 602-605,1986.

[5] Hueckel, T. and R. Pellegrini, "Effective stress and water pressure in saturated clays during heating–cooling cycles". Canadian Geotechnical Journal, 29(6): pp. 1095-1102, 1992.

[6] Abu-Hamdeh, N.H., "Thermal Properties of Soils as affected by Density and Water Content". Biosystems Engineering, 86(1): pp. 97-102, 2003.

[7] Abuel-Naga, H.M., D.T. Bergado, and A. Bouazza, "Thermally induced volume change and excess pore water pressure of soft Bangkok clay". Engineering Geology, 89(1-2): pp. 144-154, 2007.

[8] Abuel-Naga, H.M., D.T. Bergado, and B.F. Lim, "Effect of Temperature on Shear Strength and Yielding Behavior of Soft Bangkok Clay". Soils and Foundations, 47(3): pp. 423-436, 2007.

[9] Hueckel, T., B. François, and L. Laloui, "Explaining thermal failure in saturated clays". Géotechnique, 59(3): pp. 197-212, 2009.

[10] Bai, B. and Z. Su, "Thermal responses of saturated silty clay during repeated heating–cooling processes". Transport in porous media, 93(1): pp. 1-11, 2012.

[11] Mohajerani, M., et al., "A laboratory investigation of thermally induced pore pressures in the Callovo-Oxfordian claystone". International Journal of Rock Mechanics and Mining Sciences, 52: pp. 112-121, 2012.

[12] Gu, K., et al., "A study of the effect of temperature on the structural strength of a clayey soil using a micropenetrometer". Bulletin of Engineering Geology and the Environment, 73(3): pp. 747-758, 2013.

[13] Pineda, J.A., et al., "Characterisation of Ballina clay". Géotechnique, 66(7): pp. 556-577, 2016.

[14] Kelly, R.B., et al., "Site characterisation for the Ballina field testing facility". Géotechnique, 67(4): pp. 279-300, 2017.

[15] Diracdelta.co.uk "Science and Engineering Encyclopedia". Dirac Delta Consultants Ltd, Warwick, England 2007.

[16] Dobrosavljević A S, Maglić K D. "Measurements of specific heat and electrical resistivity of austenitic stainless steel (St. 1.4970) in the range 300–1500 K by pulse calorimetry". International journal of thermophysics, 13(1): pp. 57-64, 1992.

[17] Ahrens C D. Meteorology today: an introduction to weather, climate, and the environment. Belmont, 2012.

[18] Ji C, Qin Z, Dubey S, et al. "Three-dimensional transient numerical study on latent heat thermal storage for waste heat recovery from a low temperature gas flow". Applied Energy, 205: pp. 1-12, 2017.

[19] Lloret A, Vaunat J. "Thermo-hydro-mechanical behaviour of two deep belgian clay formations: boom and ypresian clays". [D]. Universitat Politècnica de Catalunya (UPC), 2011.

[20] Abu-Hamdeh N H. "Thermal properties of soils as affected by density and water content". Biosystems engineering, 86(1): pp. 97-102, 2003.

[21] Kaye, George William Clarkson; Laby,Thomas Howell. "Mechanical properties of materials". Kaye and Laby Tables of Physical and Chemical Constants. National Physical Laboratory. 2013.

[22] Jiang W, Liu Z, Gong J M, et al. "Numerical simulation to study the effect of repair width on residual stresses of a stainless steel clad plate". International Journal of Pressure Vessels and Piping, 87(8): pp. 457-463, 2010.

[23] McKetta, John J (ed.). "Encyclopedia of Chemical Processing and Design". 67. New York: Marcel Dekker. 1999

[24] Mitchell, J.K. and K. Soga, "Fundamentals of soil behavior". Vol. 3. 2005: John Wiley & Sons Hoboken, NJ.